Artifacts caused by titanium implants in CBCT images of the mandible: an experimental study

Karolina Aparecida Castilho Fardim, DDS, MSc ■ Alessiana Helena Machado, DDS, MSc
Neuza Maria Souza Picorelli Assis, DDS, MSc, PhD ■ Bruno Salles Sotto-Maior, DDS, MSc, PhD
Letícia Queiroz Mauad, DDS, MSc ■ Karina Lopes Devito, DDS, PhD

This study evaluated the quantity of metal artifacts produced by dental implants placed in different mandibular regions using various cone beam computed tomography (CBCT) protocols. Titanium implants were placed in 4 regions (incisor, canine, premolar, and molar) of an artificial mandible and subjected to CBCT examinations with the mandibular model placed in different positions within the field of view (FOV) and imaged with different FOV and voxel sizes. An axial section of the cervical region of each implant was selected for artifact quantification. The artifacts were measured by normalizing the actual standard deviation (ASD) of the voxel values. Kruskal-Wallis and Student-Newman-Keuls tests were used to compare the tooth regions and the different positions of the mandible. The Wilcoxon test was used to compare changes in FOV and voxel size. The intraobserver agreement was calculated using the intraclass correlation coefficient. The significance level was 5%. The incisor region showed significantly more artifacts than other regions ($P = 0.0315$). No statistically significant difference was found when the position of the mandible varied within the FOV ($P = 0.7418$). Smaller FOV and smaller voxels produced more artifacts ($P < 0.0001$). The quantity of metal artifacts was affected by FOV and voxel size as well as by anatomical region. Variation of the mandible location within the FOV did not affect the artifacts as defined by the normalized ASD of the voxel values.

Received: October 25, 2020
Accepted: March 15, 2021

Keywords: artifacts, cone beam computed tomography, dental implants, image enhancement

Cone beam computed tomography (CBCT) is widely used in dentistry, especially for implants, and serves as a useful tool for diagnosis and treatment planning. The images produced by CBCT allow the identification of anatomical structures, morphology, and bone dimensions.[1-3] Its use is mainly associated with specific postoperative complications (such as neurovascular trauma) and follow-up of complex surgical procedures, but CBCT can be used in the postoperative follow-up period for bone regeneration monitoring and evaluation of possible marginal bone loss as a method of 3-dimensional examination.[2,3] However, in regions with implants, metal artifacts can appear, affecting CBCT image quality.[3-5]

An image artifact is any distortion or error observed in the reconstructed data that is not present in the object under investigation.[2,6,7] In general, when a polychromatic X-ray beam passes through an object, more low-energy photons than high-energy photons are absorbed, resulting in increased mean energy and consequently in the phenomenon known as *beam hardening*. This phenomenon is intensified by the presence of materials with a high physical density, such as metals.[1,8,9]

Artifacts from metallic materials contribute to the inhomogeneity of gray values in CBCT images because they cause nonlinear attenuation of the radiation, resulting in variation in the mean X-ray beam energy.[10,11] During image reconstruction, this nonlinear attenuation affects the image quality in several ways, ranging from bright streaks radiating from the metallic object, to dark areas near it, to the complete loss of information between adjacent dense objects, which may compromise diagnosis and lead to false-positive and/or false-negative interpretations.[2,8,10,12-15]

When present in the irradiated region, dental implants can affect the tomographic image via the formation of artifacts, which can interfere with the visualization and evaluation of the peri-implant bone.[2,12,13,16,17] Studies suggest that artifact formation can be affected by the object's position within the field of view (FOV), the FOV size, the voxel size (image resolution), and adjacent anatomical structures.[10,17-19] However, no consensus is available regarding the extent to which these factors contribute to the formation of artifacts generated by the presence of dental implants. Therefore, the objective of this study was to evaluate the quantity of metal artifacts produced by dental implants placed in different mandibular regions and imaged with different CBCT protocols (variations in FOV size, voxel size, and positioning of the object within the FOV).

Methods

This cross-sectional experimental study used four 3.75 × 13.00-mm external hexagon titanium implants (Strong SW Externo,

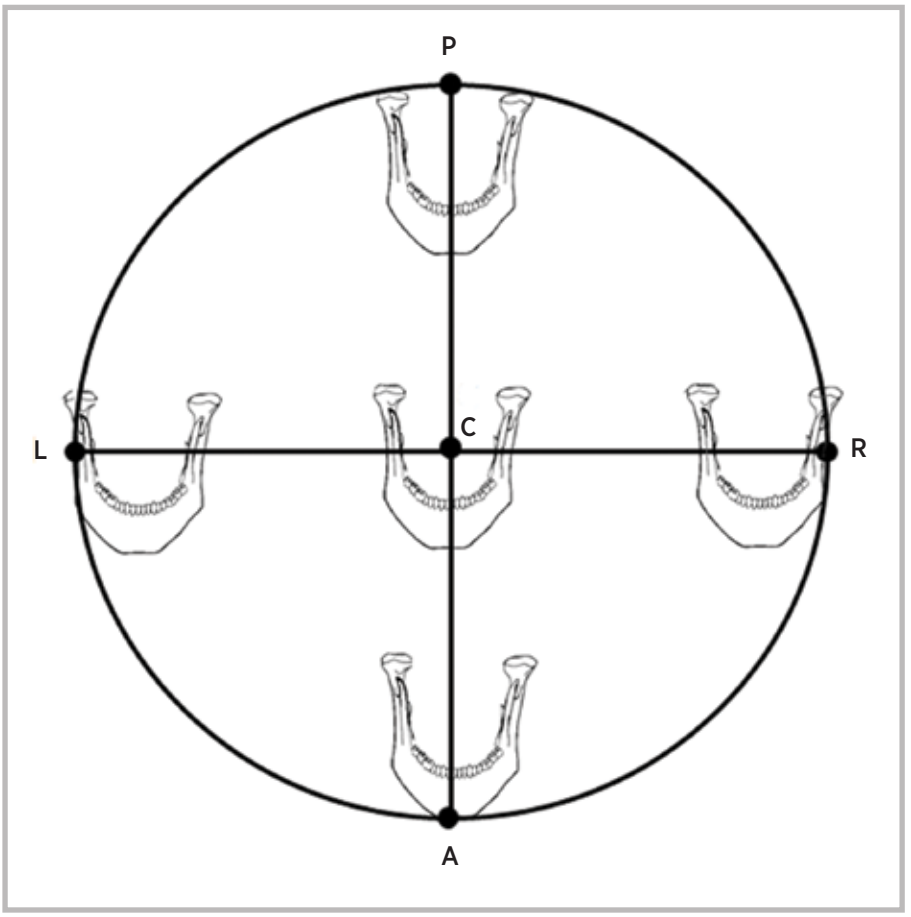

Fig 1. Five positions of the mandibular model within the field of view in the cone beam computed tomographic (CBCT) study. C, central; A, anterior; P, posterior; L, left; R, right.

S.I.N.). These implants were placed in a polyurethane and barium mandibular model (Nacional Ossos) that provided a radiographic density similar to mandibular bone. The outer surface of the mandible was covered with 15-mm-thick utility wax (Technew) for soft tissue simulation. Prior to CBCT, an implant was placed in 1 of 4 regions (incisor, canine, premolar, or molar) for evaluation; that is, the mandible had only 1 implant placed at a time during the image acquisitions.

The mandible was subjected to a total of 80 CBCT image acquisitions (i-Cat Next Generation scanner, KaVo) at 120 kV, 8 mA, and 360° rotation. The acquisitions were performed while the position of the mandible was varied within the FOV (central, anterior, posterior, right, or left) and with variations in the size of the FOV (6 × 13 or 12 × 13 cm) and voxels (0.25 or 0.30 mm). Each of the implants placed in a specific region was scanned 20 times.

The locations of the mandible within the FOV were based on the imaging method used by Valizadeh et al.[20] The mandible was assessed at 5 locations, including the central position and the 6 o'clock (the most anterior part of the FOV), 12 o'clock (the most posterior part of the FOV), 3 o'clock (the right-most part of the FOV), and 9 o'clock (the left-most part of the FOV) positions (Fig 1).[20]

After acquisition of the images, uncompressed axial images were viewed in DICOM (Digital Imaging and Communications in Medicine) format, and ImageJ software (version 1.51, National Institutes of Health) was used to select the cervical section of each implant, which is the most common region of peri-implant bone loss and where the artifacts in the present study were quantified. A standard cervical section was defined as the section located 3 mm from the base of the implant.

ImageJ software was also used to quantify the metal artifacts. A circular region of interest with a 10-mm diameter was constructed in the previously selected cervical section. This region of interest covered the entire implant region and part of the surrounding mandible, and the center of the region of interest coincided with the center of the implant. The artifacts present in each selected region of interest were quantified based on the method described by Pauwels et al.[10] ImageJ software was also used to determine the minimum and maximum grayscale values required to calculate the actual standard deviation (ASD) using the Analyze-Histogram tool. The ASD was calculated in Excel 2010 (Microsoft).

The maximum theoretical standard deviation (TSD) was calculated based on a 16-bit scale (65,536 gray values), in accordance with the characteristics of the images generated by the CBCT scanner. As half of the voxels of an image are black and half are white, the maximum TSD should be exactly half of the gray values of a particular image. Therefore, the value of

Table 1. Metal artifacts produced by different mandible positions in CBCT images with a small FOV (6 × 13 cm).

Region	Normalized ASD, %				
	Central	Anterior	Posterior	Right	Left
Voxel size: 0.25 mm (n = 4 per position per region)					
Incisor	21.08	21.61	22.89	20.68	21.77
Canine	19.73	19.38	19.63	18.23	19.48
Premolar	19.90	19.03	20.12	19.78	20.12
Molar	19.70	19.12	19.37	19.17	19.53
Voxel size: 0.30 mm (n = 4 per position per region)					
Incisor	16.62	17.01	17.40	16.40	16.24
Canine	15.49	15.59	15.51	15.09	15.99
Premolar	15.54	15.46	15.59	14.51	15.59
Molar	15.97	15.99	15.62	15.61	15.36

Abbreviations: ASD, actual standard deviation; CBCT, cone beam computed tomography; FOV, field of view.

Table 2. Metal artifacts produced by different mandible positions in CBCT images with a large FOV (12 × 13 cm).

Region	Normalized ASD, %				
	Central	Anterior	Posterior	Right	Left
Voxel size: 0.25 mm (n = 4 per position per region)					
Incisor	20.81	20.85	20.88	19.66	19.54
Canine	18.21	17.81	18.98	17.33	18.04
Premolar	19.43	18.58	20.59	18.79	19.08
Molar	18.32	18.51	18.54	17.92	19.88
Voxel size: 0.30 mm (n = 4 per position per region)					
Incisor	20.61	15.45	15.70	15.73	14.26
Canine	14.56	14.35	15.78	13.84	14.12
Premolar	14.72	14.80	15.78	14.41	15.12
Molar	15.27	14.93	13.59	14.46	16.29

Abbreviations: ASD, actual standard deviation; CBCT, cone beam computed tomography; field of view.

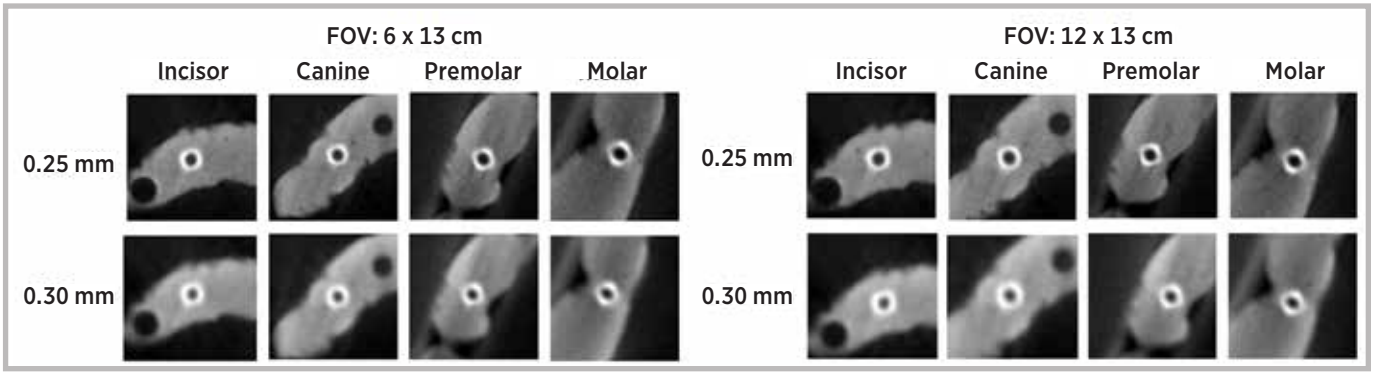

Fig 2. Examples of metal artifacts in CBCT images of dental implants. FOV, field of view.

32,768 shades of gray was adopted, and the ASD was converted into a percentage of the maximum TSD (ie, the normalized ASD), whereby higher values indicated more pronounced artifacts. The calculation was performed as follows[10]:

(ASD/maximum TSD) × 100 = quantification of artifacts

The CBCT examination, selection of the cervical section of each implant, and artifact quantification were performed by a single examiner (K.A.C.F.), who was a radiologist with experience in CBCT images. To measure the reproducibility of the method, 20% of the examinations were evaluated at 2 different times, 2 weeks apart, to calculate intraobserver agreement.

The obtained data were statistically analyzed using SPSS software (version 21.0, IBM). The significance level adopted was 5% ($P < 0.05$). Kruskal-Wallis and Student-Newman-Keuls tests were used to compare the tooth regions and the different positions of the mandible within the FOV. Wilcoxon test was used to compare variations in the FOV and voxel sizes. The level of intraobserver agreement was calculated using the intraclass correlation coefficient.

Results

Excellent intraobserver reproducibility for artifact quantification was observed (intraclass correlation coefficient = 0.9927; $P < 0.0001$). Table 1 shows the normalized ASD values of artifacts found in the CBCT images of dental implants placed in different regions and with the mandible in different locations of the small FOV. Table 2 shows the normalized ASD values in CBCTs obtained with a large FOV. Figure 2 shows examples of axial slices of the implants and their respective artifacts.

When the normalized ASDs of the artifacts were compared among the 4 tooth regions (incisor, canine, premolar, and molar), the incisor region had a significantly higher value than the other regions ($P = 0.0315$) (Table 3). Comparison of the quantities of artifacts produced at different positions of the mandible within the FOV revealed no statistically significant differences ($P = 0.7418$) (Table 4). However, comparison of the data for CBCT images with different FOV revealed that the smaller FOV produced more artifacts ($P < 0.0001$) (Table 5). In addition, when images produced with different resolutions were compared, it was found that the smaller voxels produced more artifacts ($P < 0.0001$) (Table 5).

Table 3. Metal artifacts produced by different mandibular implant regions in CBCT images (n = 20 per region).

Region	Normalized ASD, %		*P*
	Mean (SD)	Median	
Incisor	18.76 (2.64)	19.60[a]	0.0315
Canine	16.86 (2.03)	16.66[b]	
Premolar	17.35 (2.32)	17.18[b]	
Molar	17.16 (2.02)	17.10[b]	

Abbreviations: ASD, actual standard deviation; CBCT, cone beam computed tomography.

Different superscript letters indicate a statistically significant difference in median values ($P < 0.05$; Kruskal-Wallis and Student-Newman-Keuls tests).

Table 4. Metal artifacts produced at different mandibular positions within the CBCT FOV (n = 16 per position).

Position	Normalized ASD, %		*P*
	Mean (SD)	Median	
Central	17.87 (2.36)	18.26	0.7418[a]
Anterior	17.40 (2.26)	17.41	
Posterior	17.87 (2.60)	17.97	
Right	16.98 (2.24)	16.86	
Left	17.53 (2.40)	17.17	

Abbreviations: ASD, actual standard deviation; CBCT, cone beam computed tomography; FOV, field of view.

[a]No statistically significant differences in median values ($P > 0.05$; Kruskal-Wallis test).

Discussion

Cone beam computed tomography has become an indispensable diagnostic modality in dental practice, especially for treatment planning of dental implants.[3,14,21] However, the presence of objects with a high physical density, such as titanium dental implants, within the FOV can lead to the formation of metal artifacts. Due to their high atomic number, dental implants and other metallic objects within the FOV absorb a greater number of low-energy X-ray photons during image acquisition, increasing the mean energy of the X-ray beam and thereby producing beam hardening.[2,10,14,18,20] Other artifacts often caused by metal objects include extinction and exponential edge gradient effect artifacts.[7]

Although the postoperative use of CBCT in implant dentistry represents a minority of applications and should be restricted to specific situations, metal artifacts can affect image quality and are detrimental to the diagnosis of pathologic conditions such as fenestrations or peri-implant dehiscence.[3,14,16,18,19] In the present study, the SD values of the voxels were used to quantify the metal artifacts produced by titanium dental implants in CBCT images under different conditions. The studied conditions represented differences in factors that contribute to variations in gray values, such as anatomical regions, the position of the object within the FOV, and the sizes of the FOV and voxel.[18,22]

Analysis of the resulting data revealed that the gray values were not uniform across the entire mandible. When the numbers of metal artifacts in the various anatomical regions (incisor, canine, premolar, and molar) were compared, a significantly greater number of artifacts was observed in the incisor region, a finding that is consistent with the results of previous studies.[18,19] The variations in gray values among the different regions are most likely due to differences in mandibular bone density and thickness.[18,19] The gray values of CBCT images are related to the attenuation of X-rays, which, when crossing thinner regions such as incisors, are not absorbed uniformly, causing higher grayscale variability.[18]

Parameters related to the protocol for acquisition of CBCT images, such as FOV size, also affected image quality. A greater number of metal artifacts was found in the acquisitions performed with a small FOV, most likely due to the number of anatomical structures located within and outside the FOV, which affects the gray values of CBCT images.[2,18,19,23] In images with a small FOV, there is a greater presence of the so-called exomass—anatomical structures located externally to the FOV (but between the X-ray source and the image receptor) that are not reconstructed during the examination and lead to increased artifact formation.[14] Katsumata et al also observed greater grayscale variability in images with a smaller FOV and found that this variation decreased in acquisitions with a larger FOV.[24] However, a larger FOV involves higher radiation doses administered to the patient. Exposing patients to higher doses is not justifiable if no significant improvement in image quality can be achieved.[25] Pauwels et al observed that, in general, protocols with higher radiation doses do not significantly reduce the number of artifacts.[10] In clinical practice, if a larger FOV is selected only to reduce the number of artifacts, then the voxel size should be increased to compensate for the radiation dose; however, image quality is reduced as a result, with lower spatial resolution.[22]

Table 5. Metal artifacts produced in CBCT images with different FOV and voxel sizes.

Size	Normalized ASD, %		*P*
	Mean (SD)	Median	
FOV (n = 40 per size)			
6 × 13 cm	17.92 (2.30)	17.81	< 0.0001[a]
12 × 13 cm	17.14 (2.34)	17.57	
Voxel (n = 40 per size)			
0.25 mm	19.55 (1.17)	19.50	< 0.0001[a]
0.30 mm	15.51 (1.16)	15.52	

Abbreviations: ASD, actual standard deviation; CBCT, cone beam computed tomography; FOV, field of view.

[a]Statistically significant difference in median values ($P < 0.05$; Wilcoxon test).

In the present study, when images produced at 2 different resolutions were compared, the smaller voxel was found to produce a greater number of artifacts. This result differs from that of Pauwels et al, who found that varying the voxel size did not affect gray values.[10] A possible explanation for the variation in the number of artifacts found for different voxel sizes may be related to image noise. Voxels of different sizes detect X-ray photons differently. A smaller voxel will not detect as many photons as a larger voxel because of the reduced signal and increased noise of the former. In turn, larger voxels can detect more energy and thus improve the signal.[17]

According to the literature, metal artifacts are also affected by the location of the object within the FOV.[20,25-27] In this study, no significant differences in the quantities of artifacts were observed when the position of the mandible within the FOV was changed from the central position to the anterior, posterior, right, or left position. Valizadeh et al assessed the diagnosis of vertical root fractures in teeth with metallic intracanal pins and concluded that the central position produced the highest sensitivity values (resulting in better diagnosis of fractures) and the 3 o'clock (right) position produced the highest specificity values (resulting in better diagnosis of healthy teeth).[20] According to Candemil et al, the mean gray values generally increase (resulting in a brighter image) at the periphery of the FOV and decrease (resulting in a darker image) in the central region of the FOV, regardless of the presence of metal objects in the exomass.[23]

An alternative method for minimizing metal artifacts is the use of metal artifact reduction algorithms. Some studies have used these artifact reduction tools to improve the diagnosis of peri-implant bone defects or root fractures.[28,29] Bechara et al reported improved image quality after application of these algorithms.[15] However, there is no consensus regarding the reliability of this tool.[1,6,10,16,28,29] It seems that metal artifact reduction solutions do not currently add diagnostic information, even if the image quality parameters are improved.[3]

The use of only a single CBCT device should be considered a limitation of the present study. In addition, other exposure factors, such as kilovolts (peak), should be investigated. Thus, to provide better image quality and achieve lower radiation doses, more research on artifact quantification with other equipment is needed to assist in the development of future generations of CBCT devices, better metal artifact reduction algorithms, and improved image processing software.

Conclusion

Within the limitations of this study, the results suggest that metal artifacts are affected by the FOV and voxel size as well as by anatomical region. Variation of the mandibular location within the FOV did not affect the artifacts as defined by the normalized ASD of the voxel values.

Author affiliations

Department of Oral Diagnosis and Surgery, School of Dentistry, São Paulo State University, Institute of Science and Technology, São José dos Campos, Brazil (Fardim); Department of Oral Diagnosis, Division of Oral Radiology, Piracicaba Dental School, University of Campinas, Piracicaba, Brazil (Machado); Department of Dental Clinic, School of Dentistry, Federal University of Juiz de Fora, Juiz de Fora, Brazil (Assis, Devito); Department of Restorative Dentistry, School of Dentistry, Federal University of Juiz de Fora, Juiz de Fora, Brazil (Sotto-Maior); Master's Program in Dentistry, School of Dentistry, Federal University of Juiz de Fora, Juiz de Fora, Brazil (Mauad).

Disclaimer

The authors report no conflicts of interest pertaining to any of the products or companies discussed in this article.

References

1. Bechara B, Alex McMahan C, Moore WS, Noujeim M, Teixeira FB, Geha H. Cone beam CT scans with and without artefact reduction in root fracture detection of endodontically treated teeth. *Dentomaxillofac Radiol*. 2013;42(5):20120245. doi:10.1259/dmfr.20120245
2. Sancho-Puchades M, Hämmerle CH, Benic GI. In vitro assessment of artifacts induced by titanium, titanium-zirconium and zirconium dioxide implants in cone-beam computed tomography. *Clin Oral Implants Res.* 2015;26(10):1222-1228.
3. Jacobs R, Salmon B, Codari M, Hassan B, Bornstein MM. Cone beam computed tomography in implant dentistry: recommendations for clinical use. *BMC Oral Health.* 2018;18(1):88. doi:10.1186/s12903-018-0523-5
4. Nagarajappa AK, Dwivedi N, Tiwari R. Artifacts: the downturn of CBCT image. *J Int Soc Prev Community Dent.* 2015;5(6):440-445.
5. Smeets R, Schöllchen M, Gauer T, et al. Artefacts in multimodal imaging of titanium, zirconium and binary titanium-zirconium alloy dental implants: an in vitro study. *Dentomaxillofac Radiol.* 2017;46(2):20160267. doi:10.1259/dmfr.20160267
6. Kamburoglu K, Kolsuz E, Murat S, Eren H, Yüksel S, Paksoy CS. Assessment of buccal marginal alveolar peri-implant and periodontal defects using a cone beam CT system with and without the application of metal artefact reduction mode. *Dentomaxillofac Radiol.* 2013;42(8):20130176. doi:10.1259/dmfr.20130176
7. Kuusisto N, Vallittu PK, Lassila LV, Huumonen S. Evaluation of intensity of artefacts in CBCT by radio-opacity of composite simulation models of implants in vitro. *Dentomaxillofac Radiol.* 2015;44(2):20140157. doi:10.1259/dmfr.20140157
8. Jaju PP, Jain M, Singh A, Gupta A. Artefacts in cone beam CT. *Open J Stomatol.* 2013;3(5):292-297.
9. Panjnoush M, Kheirandish Y, Kashani PM, Fakhar HB, Younesi F, Mallahi M. Effect of exposure parameters on metal artifacts in cone beam computed tomography. *J Dent (Tehran).* 2016;13(3):143-150.
10. Pauwels R, Stamatakis H, Bosmans H, et al. Quantification of metal artifacts on cone beam computed tomography images. *Clin Oral Implants Res.* 2013;24(Suppl A100):94-99.
11. Moudi E, Haghanifar S, Madani Z, Bijani A, Nabavi ZS. The effect of metal artifacts on the identification of vertical root fractures using different fields of view in cone-beam computed tomography. *Imaging Sci Dent.* 2015;45(3):147-151.
12. Kratz B, Weyers I, Buzug TM. A fully 3D approach for metal artifact reduction in computed tomography. *Med Phys.* 2012;39(11):7042-7054.
13. Esmaeili F, Johari M, Haddadi P. Beam hardening artifacts by dental implants: comparison of cone-beam and 64-slice computed tomography scanners. *Dent Res J (Isfahan).* 2013;10(3):376-381.
14. Schulze RK, Berndt D, d'Hoedt B. On cone-beam computed tomography artifacts induced by titanium implants. *Clin Oral Implants Res.* 2010;21(1):100-107.
15. Bechara BB, Moore WS, McMahan CA, Noujeim M. Metal artefact reduction with cone beam CT: an in vitro study. *Dentomaxillofac Radiol.* 2012;41(3):248-253.
16. Parsa A, Ibrahim N, Hassan B, Syriopoulos K, van der Stelt P. Assessment of metal artefact reduction around dental titanium implants in cone beam CT. *Dentomaxillofac Radiol.* 2014;43(7):20140019. doi:10.1259/dmfr.20140019
17. Vasconcelos TV, Bechara BB, McMahan CA, Freitas DQ, Noujeim M. Evaluation of artifacts generated by zirconium implants in cone-beam computed tomography images. *Oral Surg Oral Med Oral Pathol Oral Radiol.* 2017;123(2):265-272.
18. Oliveira ML, Tosoni GM, Lindsey DH, Mendoza K, Tetradis S, Mallya SM. Influence of anatomical location on CT numbers in cone beam computed tomography. *Oral Surg Oral Med Oral Pathol Oral Radiol.* 2013;115(4):558-564.
19. Machado AH, Fardim KAC, de Souza CF, Sotto-Maior BS, Assis NMSP, Devito KL. Effect of anatomical region on the formation of metal artefacts produced by dental implants in cone beam computed tomographic images. *Dentomaxillofac Radiol.* 2018;47(3):20170281. doi:10.1259/dmfr.20170281
20. Valizadeh S, Vasegh Z, Rezapanah S, Safi Y, Khaeazifard MJ. Effect of object position in cone beam computed tomography field of view for detection of root fractures in teeth with intracanal posts. *Iran J Radiol.* 2015;12(4):e25272. doi:10.5812/iranjradiol.25272
21. Benic GI, Sancho-Puchades M, Jung RE, Deyhle H, Hämmerle CH. In vitro assessment of artifacts induced by titanium dental implants in cone beam computed tomography. *Clin Oral Implants Res.* 2013;24(4):378-383.

22. Queiroz PM, Santaella GM, da Paz TD, Freitas DQ. Evaluation of a metal artefact reduction tool on different positions of a metal object in the FOV. *Dentomaxillofac Radiol.* 2017;46(3):20160366. doi:10.1259/dmfr.20160366
23. Candemil AP, Salmon B, Freitas DQ, Haiter-Neto F, Oliveira ML. Distribution of metal artifacts arising from the exomass in small field-of-view cone beam computed tomography scans. *Oral Surg Oral Med Oral Pathol Oral Radiol.* 2020;130(1):116-125.
24. Katsumata A, Hirukawa A, Okumura S, et al. Relationship between density variability and imaging volume size in cone-beam computerized tomographic scanning of the maxillofacial region: an in vitro study. *Oral Surg Oral Med Oral Pathol Oral Radiol Endod.* 2009;107(3):420-425.
25. Pauwels R, Jacobs R, Bogaerts R, Bosmans H, Panmekiate S. Reduction of scatter-induced image noise in cone beam computed tomography: effect of field of view size and position. *Oral Surg Oral Med Oral Pathol Oral Radiol.* 2016;121(2):188-195.
26. SEDENTEXCT project. Radiation protection, No. 172: Cone beam CT for dental and maxillofacial radiology. Evidence-based guidelines. Luxembourg: European Commission Directorate-General for Energy; 2012. Accessed October 27, 2021. http://www.sedentexct.eu/files/radiation_protection_172.pdf
27. Taylor C. Evaluation of the effects of positioning and configuration on contrast-to-noise ratio in the quality control of a 3D Accuitomo 170 dental CBCT system. *Dentomaxillofac Radiol.* 2016;45(5):20150430. doi:10.1259/dmfr.20150430
28. de-Azevedo-Vaz SL, Peyneau PD, Ramirez-Sotelo LR, Vasconcelos Kde F, Campos PS, Haiter-Neto F. Efficacy of a cone beam computed tomography metal artifact reduction algorithm for the detection of peri-implant fenestrations and dehiscences. *Oral Surg Oral Med Oral Pathol Oral Radiol.* 2016;121(5):550-556.
29. de Rezende Barbosa GL, Sousa Melo SL, Alencar PN, Nascimento MC, Almeida SM. Performance of an artefact reduction algorithm in the diagnosis of in vitro vertical root fracture in four different root filling conditions on CBCT images. *Int Endod J.* 2016;49(5):500-508.